

Strong variation of electrostrictive coupling near an intermediate temperature of relaxor ferroelectrics

F. Craciun

Istituto dei Sistemi Complessi, CNR-ISC, Area della Ricerca di Roma Tor Vergata, Via del Fosso del Cavaliere 100, I-00133 Roma, Italy

(Received 12 March 2010; revised manuscript received 6 May 2010; published 28 May 2010)

A sudden increase in the electrostrictive coefficient Q_{13} when temperature decreases is seen in three different types of ferroelectric relaxors (PLZT 9/65/35, PLZT 22/20/80, and PMN-PT) starting from ~ 50 K above the dielectric permittivity maximum temperature, T_m . The temperature dependence is attributed to the softening of the quasilocal mode occurring near dopants or charge-transfer sites. The steep increase when the temperature decreases could be related to the transition of polar nanoregions from dynamic to quasistatic regime, which introduces an intermediate temperature scale T^* [W. Dmowski, S. B. Vakhrushev, I.-K. Jeong, M. P. Hehlen, F. Trouw, and T. Egami, Phys. Rev. Lett. **100**, 137602 (2008); B. Dkhil, P. Gemeiner, A. Al-Barakaty, L. Bellaiche, E. Dul'kin, E. Mojaev, and M. Roth, Phys. Rev. B **80**, 064103 (2009)], besides Burns temperature T_B and freezing temperature T_f . Possible consequences for nonequilibrium phenomena, including high-temperature memory found in relaxors, are conjectured.

DOI: 10.1103/PhysRevB.81.184111

PACS number(s): 77.80.Jk, 75.10.Nr, 77.65.Bn, 77.84.Cg

Remarkable advance has been made over the past several years in the understanding of the properties of relaxor ferroelectrics.^{1–15} Enhanced resolution performance of the investigation techniques have shown that the local structure of these compounds is very different from the average crystallographic one.^{13–19} Different models based on quenched random fields due to compositional fluctuations,² spin-glass state induced by interactions among polar clusters,¹ random fields¹² or spherical random bonds and random fields³ have been developed in order to understand their properties. Relaxor ferroelectrics, mostly of the perovskite type, have disorder in the cation sublattices that inhibits the formation of long-range order and are in many aspects similar to spin glasses, with freezing of the polarization fluctuations and nonequilibrium phenomena such as aging, rejuvenation, and memory.^{20–22} Below the so-called Burns temperature T_B , fluctuating polar clusters of nanometer size start forming and, on cooling at lower temperatures,²³ a competition between growth and freezing of these polar nanoregions (PNR) gives rise to the typical frequency dispersion in the ac susceptibility and to a broad permittivity maximum at a frequency-dependent temperature $T_m(\omega)$. The existence of an intermediate temperature scale T^* , in between T_B and T_m , related to a transition of PNRs from dynamic to quasistatic regime, has been recently established.^{19,24–28} The characteristic relaxation time τ deduced from the relationship $\omega\tau \approx 1$ at the maximum $T_m(\omega)$ diverges at a finite temperature approximately following Vogel-Fulcher law $\tau = \tau_0 e^{E/(T-T_f)}$ with T_f freezing or glass transition temperature.²⁹ Nonequilibrium phenomena such as aging are rather frequent in solids with disorder, but rejuvenation and especially memory are considered as peculiar of the frozen spin-glass state,³⁰ and theoretical models for them rely on a proliferation of hierarchically organized metastable states below T_f (Ref. 31) or the vanishing of the barriers between these metastable states above T_f .³² However, it has been shown that PLZT has even memory of multiple aging stages above T_f ,^{22,33} which is an indication that in this material some mechanism of hierarchical organized correlations intrinsic of the relaxor state is in-

volved also above the relaxor transition, rather than marginally mobile defects.³³ The motivation for the present research was given by the necessity to look for a possible mechanism that could be responsible for the behavior above T_f .

The materials investigated here are: (Pb/La)(Zr/Ti)O₃ with (a) La concentration 0.09 and Zr/Ti ratio 65/35 (PLZT 9/65/35); (b) La concentration 0.22 and Zr/Ti ratio 20/80 (PLZT 22/20/80), and (c) 0.9 Pb(Mg_{1/3}Nb_{2/3})O₃-0.1 PbTiO₃ (PMN-PT). The preparation of PLZT-type samples was described in Refs. 22, 33, and 34 while PMN-PT was purchased from TRS ceramics. Previous results obtained from structural, dielectric, and anelastic measurements on these samples have been reported in Refs. 22 and 33–35. The samples have been rectangular bars with dimensions 45 × 4 × 0.45 mm³ (PLZT 9/65/35), 30 × 4 × 0.63 mm³ (PLZT 22/20/80), and 45 × 4 × 0.5 mm³ (PMN-PT).

The dielectric ac permittivity $\epsilon = \epsilon' - i\epsilon''$ was measured with an HP 4194 A impedance bridge with a four wire probe and a signal level of 0.5 V/mm in the sweeping frequency mode while a dc bias field with amplitude E_0 in the range 1–80 V/mm was applied along the shortest dimension. The measurements have been made at different temperatures in the range 300–580 K. Typical results of $\epsilon''(\omega)$ for the PMN-PT sample are shown in Fig. 1.

Following the results of the model developed in Ref. 36, the real and imaginary permittivity can be written as

$$\epsilon'(\omega) = \frac{\epsilon_s + \epsilon_\infty \omega^2 \tau^2}{\omega^2 \tau^2 + 1} - \frac{1}{s_{11}^E} \frac{4E_0^2 M_{13}^2}{\omega^2 \tau^2 + 1} (1 - Y_r - \omega \tau Y_i), \quad (1)$$

$$\epsilon''(\omega) = \frac{(\epsilon_s - \epsilon_\infty) \omega \tau}{\omega^2 \tau^2 + 1} - \frac{1}{s_{11}^E} \frac{4E_0^2 M_{13}^2}{\omega^2 \tau^2 + 1} (\omega \tau - \omega \tau Y_r + Y_i) \quad (2)$$

with ϵ_s and ϵ_∞ the static and infinite frequency limit permittivity, respectively, s_{11}^E the elastic compliance at constant electric field and M_{13} the appropriate electrostrictive coefficient that couples electric field on x_3 direction to strain on the longest x_1 direction.

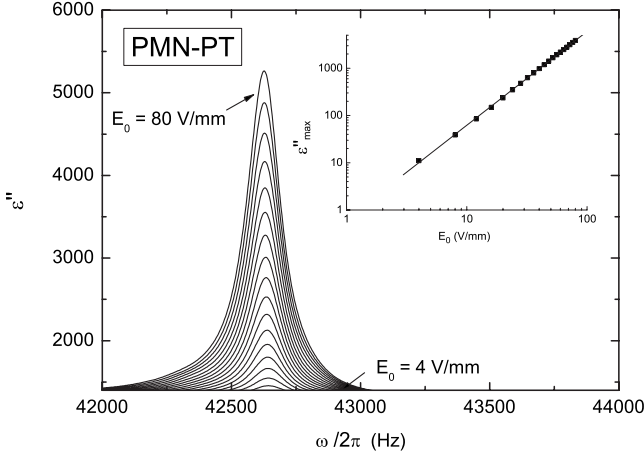


FIG. 1. $\epsilon''(\omega, E_0)$ for PMN-PT measured at $T \approx 300$ K. E_0 varies between 0 and 80 V/mm with a step of 4 V/mm. The inset shows the dependence of ϵ''_{max} on E_0 in a log-log scale. The amplitude of $\epsilon'' \sim E_0^2$.

The functions Y_r and Y_i are proportional to the mechanical strain and are given by

$$Y_r = \frac{\theta \sin \theta \cos \theta + \beta \sinh \beta \cosh \beta}{(\theta^2 + \beta^2)(\cos^2 \theta + \sinh^2 \beta)}, \quad Y_i = \frac{\theta \sinh \beta \cosh \beta - \beta \sin \theta \cos \theta}{(\theta^2 + \beta^2)(\cos^2 \theta + \sinh^2 \beta)}, \quad (3)$$

where $\theta = \frac{\omega l}{2V}$, $\beta = \frac{\eta \omega^2 l}{4V^3 \rho}$, l and ρ are the bar length and density, V is the acoustic wave velocity, and η the viscosity which is related to the acoustic attenuation coefficient α by the expression $\alpha = \frac{\eta \omega^2}{2V^3 \rho}$.³⁶

The model has been developed for the simple case of Debye relaxation and its validity is limited to the range $\omega\tau \leq 1$ in which the reorientation-induced stress fully relaxes but, however, can be applied also for more complex relaxation spectrum.³⁶ The relaxation time τ for the three samples has been calculated for different temperatures from the

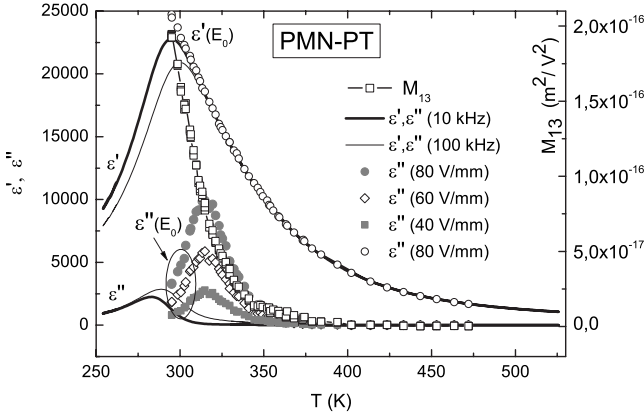


FIG. 2. Temperature dependence of $\epsilon''_{max}(E_0)$ and of the electrostrictive coefficient M_{13} , for PMN-PT. $E_0 = 0, 40, 60$, and 80 V/mm. ϵ' and ϵ'' measured in a different run without bias field at 10 and 100 kHz are also shown.

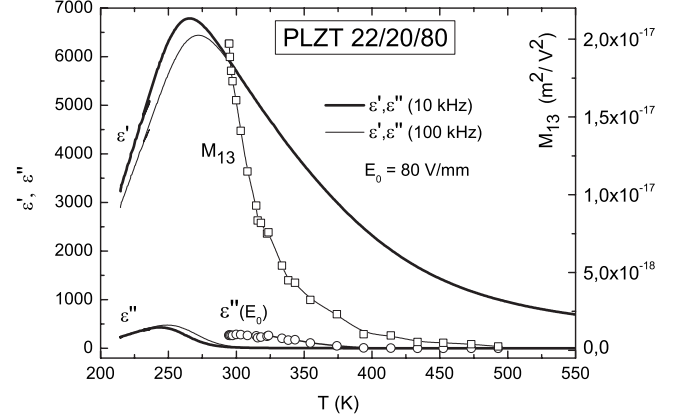


FIG. 3. Temperature dependence of $\epsilon''_{max}(E_0)$ at $E_0 = 80$ V/mm and of the electrostrictive coefficient M_{13} , for PLZT 22/20/80. ϵ' and ϵ'' measured without bias field at 10 and 100 kHz are also displayed.

Vogel-Fulcher law $\tau = \tau_0 e^{E/(T-T_f)}$ with τ_0 , E , and T_f listed below for each sample: (a) $\tau_0 = 2.1 \times 10^{-11}$, $E = 449$ K, $T_f = 320.5$ K (PLZT 9/65/35);²² (b) $\tau_0 = 1 \times 10^{-14}$, $E = 1450$ K, $T_f = 190$ K (PLZT 22/20/80);³⁴ (c) $\tau_0 = 1.98 \times 10^{-13}$, $E = 649$ K, $T_f = 247.3$ K (PMN-PT).³⁵ Frequency ω was swept around the frequency of mechanical resonance for each sample (about 42 kHz for PLZT 9/65/35 and PMN-PT and about 70 kHz for PLZT 22/20/80). The temperature region for each sample was restricted from below in order to have the condition $\omega\tau \leq 1$ fulfilled. V and s_{11}^E have been calculated by using simple relationships³⁶ while acoustic attenuation coefficient $\alpha = \frac{\omega}{V} Q^{-1}$ has been calculated at each temperature by using the values of mechanical quality factor $Q(T)$ reported in Refs. 22 and 33–35. The electrostrictive coefficient M_{13} calculated from Eq. (2) for PMN-PT is presented in Fig. 2, together with ϵ' and ϵ'' at $E=0, 40, 60$, and 80 V/mm. The curves at zero-bias field (continuous lines) have been measured at 10 and 100 kHz, in a previous run. Similar results obtained for PLZT samples are shown in Figs. 3 and 4. It can be observed that in all cases M_{13} has a marked increase with temperature decreasing, starting from about 50 K above T_m .

Within the framework of thermodynamics of crystals,

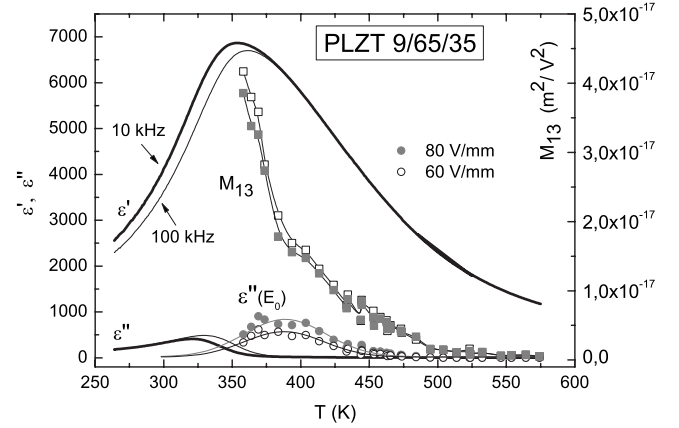


FIG. 4. The same as in Figs. 2 and 3, for PLZT 9/65/35, at $E_0 = 60$ and 80 V/mm.

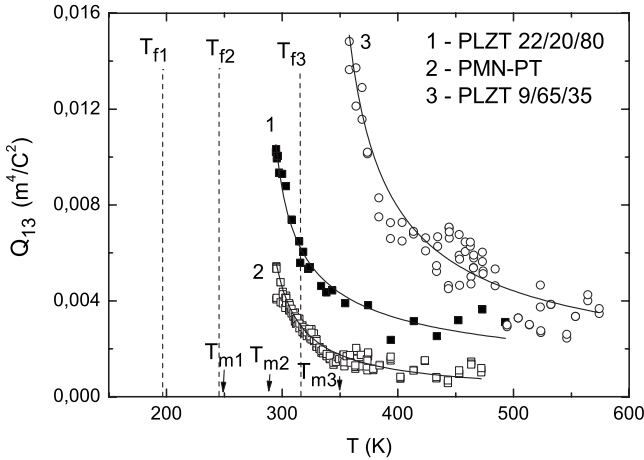


FIG. 5. The electrostrictive coefficient Q_{13} for the three different relaxor systems. The values of the corresponding temperatures of freezing T_f and of the dielectric permittivity maximum T_m are marked by dashed lines and arrows, respectively.

nonlinear effects can be described by taking into account terms of the third degree or higher in the expansions of thermodynamic potentials. So for the thermodynamic potential Φ the following expansion should be used:³⁷

$$\Phi = \Phi_0 - \frac{1}{2} \varepsilon_{ij} E_i E_j - d_{i\lambda} E_i \sigma_\lambda - \frac{1}{2} s_{\lambda\nu} \sigma_\lambda \sigma_\nu - M_{ik\lambda} E_i E_k \sigma_\lambda - \dots, \quad (4)$$

where the second, third, and fourth terms are the electric, piezoelectric, and elastic parts, respectively.

The coefficients of electrostriction M describe small corrections to the converse piezoelectric effect in piezoelectric crystals while for crystals of nonpiezoelectric classes and for isotropic bodies all strain caused by the action of an electric field reduces to electrostriction. The electrostrictive coefficients are defined by the phenomenological relation $e_{ij} = M_{ijkl} E_k E_l = Q_{ijkl} P_k P_l$ (in the extended notation), where e_{ij} is the strain. For a relaxor, the two electrostrictive coefficients M_{13} and Q_{13} are related by the simple formula $M_{13} = Q_{13} \varepsilon^2$. The obtained Q_{13} coefficients for the three samples are represented in Fig. 5. On the same graph the values of the corresponding T_m and T_f have been marked by arrows and dashed lines, respectively. It can be observed that Q_{13} coefficients increase with temperature decreasing, above T_m and much above T_f , although the obvious dielectric permittivity dependence has been extracted. It is generally believed that electrostrictive coefficients do not vary with temperature,³⁸ however such variation has been reported for PMN and PMN-PT,³⁹ and recently for some ferroelectric perovskites.^{40,41}

A model for the electrostrictive coefficients in terms of microscopic parameters has been proposed in Ref. 42. Within this approach it is assumed that the main mechanism of electrostriction is due to the charge transfer and active ion displacements occurring in correlated pairs or triads of Nb and O ions and their strong interaction with lattice distortions. A localized O-Nb-O triad is part of a small cluster of ions in the

Mg-rich region with a Nb ion at its center. The concentration c_0 of localized triads is controlled by chemical fluctuations, e.g., Mg/Nb local ratio in PMN-type relaxors. A second mechanism is based on quasilocal vibrations due to substitutional impurities, which interact with the soft lattice polarization and the elastic strains. The total energy of the triads O-Nb-O is written in terms of electrostrictive and elastic deformation energy and, by minimization, a system of equations for the main elastic strains in terms of polarization are obtained and used to extract the electrostrictive coefficients. It has been found that Q_{13} is of the order of magnitude

$$Q_{13} = \frac{c_0}{6v_0 C_{11}} \frac{|\tilde{B}_E| B^2}{K^2}, \quad (5)$$

where B and \tilde{B}_E are the coupling of the quasilocal stretching mode to polarization and to lattice vibrations, respectively, $K = m_0 \omega_0^2$ with m_0 and ω_0 the effective mass and frequency of the quasilocal stretching mode; v_0 is the elementary cell volume and C_{11} is the elastic constant. With the parameters used in Ref. 42 for PMN, $Q_{13} \approx -0.96 \times 10^{-2} \text{ m}^4 \text{ C}^{-2}$, which is the order of magnitude of the experimentally obtained values.³⁸ We do not know the values of the parameters in Eq. (5) for our samples, however we are more interested in the variation of the electrostrictive coefficient with temperature; therefore following the same reasoning and the approximation used in Ref. 42: $\tilde{B}_E \approx K \delta$, with parameter $\delta < 0, |\delta| < 1$, one can see that $Q_{13} \propto K^{-1} \propto \omega_0^{-2}$. Thus the main variation of Q_{13} with temperature should be introduced by the frequency of the quasilocal mode. Similar local modes near dopants or charge-transfer sites and their temperature dependence have been modeled in Ref. 10. These intrinsic local modes (ILMs) can be dopants or, e.g., Pb polarization in the oxygen cage in PMN, embedded in the (Mg/Nb)O₃ sublattice which represents the soft dielectric host matrix. The random occupation of the lattice sites by Mg²⁺ and Nb⁵⁺ ions impedes the direct coupling of ILMs to each other. The ILMs are coupled to the soft host matrix by superimposing the displacement patterns and nonlinearity is introduced in the polarizability of the system, due to local charge imbalance. The cross terms in potentials stabilize the lattice against ferroelectric softening and make ILM potential temperature dependent. The calculated dispersion relations show that the ILM splits from the transverse-optic mode at the Burns temperature T_B in the energy range of 3–4 THz and cross the transverse-acoustic mode at large q values at a much lower temperature. The transverse-optic $q=0$ mode show only little softening with decreasing temperature and a lattice instability does not occur. Similarly, the acoustic zone boundary mode remains nearly temperature independent while the squared ILM mode frequency is almost linearly dependent on temperature: $\omega_0^2 \propto T$. By substituting in Eq. (5) one obtains: $Q_{13} \propto T^{-1}$. However, when compared to experimental results in Fig. 5, this dependence is too slow (rough fitting of the curves with power law T^{-n} yields exponents between 3.5 and 4). Nevertheless the models include a few crude approximations and some parameters are not at all known.

Since curves in Fig. 5 have rather steep increase starting from about 50 K above T_m which recall the onset of a tem-

perature scale, we addressed to other experimental results on ferroelectric relaxors which display similar behavior. Thus temperature evolution of phonon anomalies and the pseudocubic unit-cell parameter for $\text{Pb}(\text{Sc}_{0.5}\text{Ta}_{0.5})\text{O}_3$ -based relaxors revealed the existence of a characteristic temperature T^* between T_B and T_m .²⁸ This temperature has been also identified by the analysis of Raman spectra on PMN, where $T^* \sim 350$ K marks the slowing down of the reorientation dynamics of PNRs, and on PZN-based relaxors.^{26,27} Moreover, acoustic emission experiments correlated with various experimental and theoretical techniques have evidenced this intermediate temperature scale in different lead-based ferroelectric relaxors with B-site disorder.^{24,25} Results from advanced structural investigation techniques led to similar conclusions. Thus dynamic pair-density function (DPDF) determined by pulsed neutron inelastic scattering¹⁹ evidenced the temperature evolution of the frequency of Pb ion off-centering in the oxygen ions cage and against Mg/Nb sublattice in PMN. While the static PDF showed that local Pb polarizations disappear above a temperature $T^* \sim 300$ K, DPDF at 450 K showed the presence of Pb and O dynamic local polarization with the characteristic frequency of about 4 THz (16 meV). Moreover DPDF integrated from 10 to 20 meV shows that local Pb polarizations extend to much higher temperatures, disappearing only around $T_B \sim 600$ K. These results have been taken as evidence for a third temperature scale T^* in relaxor ferroelectrics, in addition to T_f and T_B ; static local polarization appears below T^* , whereas between T^* and T_B local polarizations are dynamic and are less correlated with almost no distortion. It should be noticed that T^* (~ 40 K above T_m) is close to the temperature (340 K) where the intensity of the softening phonon diverges in extrapolation from high temperatures¹⁸ and also not far from the temperature (~ 400 K) where the elastic diffuse neutron-scattering intensity disappears and the intensity of the quasielastic scattering is maximum.¹⁶ The energy of the soft phonon branches involving Pb-O displacements is about 5–15 meV when the waterfall behavior is observed,¹⁸ similar

to the energy range where the anomalies evidenced by DPDF are observed. Therefore, it is believed that the resonance between the local dynamical off-centering of Pb ions and these soft phonons produces the dynamic short-range correlation in polarization, resulting in the formation of a local polarization cloud at temperatures below T_B . This resonance between the local polar moment and the soft phonons was modeled in Ref. 10 and probably is the origin of the waterfall behavior, given by the scattering of long wave phonons by the local polarization clouds.¹⁹ Below T^* dynamic local polarizations slow down sufficiently to form quasistatic polar nanoregions.¹⁹ We believe that the transition from the dynamic to quasistatic regime in PNRs formation could be at the origin of the steep increase in electrostrictive coefficient in our experiment.⁴³

We discuss now the possible implications that the intermediate temperature scale for electrostrictive coupling could have for nonequilibrium phenomena. In the last few years clear experimental evidence has been found in support of the idea that, as in the spin-glass case, the polarizing units in relaxor ferroelectrics are the same units whose interactions drive the formation of the glassy state.⁴⁴ At the transition of polar nanoregions from dynamic to quasistatic regime the electrostrictive coupling suddenly increases and coupling of polarization degree of freedom with strain is enhanced. Electrostrictive strains are one or two orders of magnitude larger than magnetostrictive strains. This could influence also non-equilibrium phenomena and induce strong differences among magnetic spin glasses and relaxor ferroelectrics. The local electrostrictive phenomena in relaxor ferroelectrics are controlled by the square of polarization of polar nanoregions. Thus electrostrictive strains act as new degrees of freedom, linked to polarization. Therefore the hierarchical organization and all the typical glassy features related to the main order parameter are conserved. We believe that this could be a possible mechanism for high-temperature memory found in relaxor ferroelectrics and up to now unexplained.

¹D. Viehland, J. F. Li, S. J. Jang, L. E. Cross, and M. Wuttig, *Phys. Rev. B* **43**, 8316 (1991).
²V. Westphal, W. Kleemann, and M. D. Glinchuk, *Phys. Rev. Lett.* **68**, 847 (1992).
³R. Pirc and R. Blinc, *Phys. Rev. B* **60**, 13470 (1999).
⁴B. E. Vugmeister and H. Rabitz, *Phys. Rev. B* **57**, 7581 (1998).
⁵E. V. Colla, E. Yu. Koroleva, N. M. Okuneva, and S. B. Vakhrushev, *Phys. Rev. Lett.* **74**, 1681 (1995).
⁶A. K. Tagantsev, *Phys. Rev. Lett.* **72**, 1100 (1994).
⁷R. Blinc, J. Dolinsk, A. Gregorovič, B. Zalar, C. Filipič, Z. Kutnjak, A. Levstik, and R. Pirc, *Phys. Rev. Lett.* **83**, 424 (1999); R. Pirc, R. Blinc, and V. Bobnar, *Phys. Rev. B* **63**, 054203 (2001).
⁸M. D. Glinchuk and R. Farhi, *J. Phys.: Condens. Matter* **8**, 6985 (1996).
⁹A. Bussmann-Holder and A. R. Bishop, *Phys. Rev. B* **70**, 184303 (2004); *J. Phys.: Condens. Matter* **16**, L313 (2004).
¹⁰A. Bussmann-Holder, A. R. Bishop, and T. Egami, *Europhys.*

Lett. **71**, 249 (2005).
¹¹A. Bussmann-Holder, H. Beige, and G. Völkel, *Phys. Rev. B* **79**, 184111 (2009).
¹²B. E. Vugmeister, *Phys. Rev. B* **73**, 174117 (2006).
¹³E. Prouzet, E. Housson, N. de Mathan, and A. Morell, *J. Phys.: Condens. Matter* **5**, 4889 (1993).
¹⁴B. Dkhil, J. M. Kiat, G. Calvarin, G. Baldinozzi, S. B. Vakhrushev, and E. Suard, *Phys. Rev. B* **65**, 024104 (2001).
¹⁵K. Hirota, S. Wakimoto, and D. E. Cox, *J. Phys. Soc. Jpn.* **75**, 111006 (2006).
¹⁶H. Hiraka, S.-H. Lee, P. M. Gehring, G. Xu, and G. Shirane, *Phys. Rev. B* **70**, 184105 (2004).
¹⁷I.-K. Jeong, T. W. Darling, J. K. Lee, Th. Proffen, R. H. Heffner, J. S. Park, K. S. Hong, W. Dmowski, and T. Egami, *Phys. Rev. Lett.* **94**, 147602 (2005).
¹⁸S. B. Vakhrushev and S. M. Shapiro, *Phys. Rev. B* **66**, 214101 (2002).
¹⁹W. Dmowski, S. B. Vakhrushev, I.-K. Jeong, M. P. Hehlen, F.

Trouw, and T. Egami, *Phys. Rev. Lett.* **100**, 137602 (2008).

²⁰E. V. Colla, L. K. Chao, and M. B. Weissman, *Phys. Rev. B* **63**, 134107 (2001).

²¹O. Kircher and R. Böhmer, *Eur. Phys. J. B* **26**, 329 (2002).

²²F. Cordero, F. Craciun, A. Franco, D. Piazza, and C. Galassi, *Phys. Rev. Lett.* **93**, 097601 (2004).

²³S. Kamba, V. Bovtun, J. Petzelt, I. Rychetsky, R. Mizaras, A. Brilingas, J. Banys, J. Grigas, and M. Kosec, *J. Phys.: Condens. Matter* **12**, 497 (2000).

²⁴B. Dkhil, P. Gemeiner, A. Al-Barakaty, L. Bellaiche, E. Dul'kin, E. Mojaev, and M. Roth, *Phys. Rev. B* **80**, 064103 (2009); M. Roth, E. Mojaev, E. Dul'kin, P. Gemeiner, and B. Dkhil, *Phys. Rev. Lett.* **98**, 265701 (2007).

²⁵E. Dul'kin, M. Roth, P.-E. Janolin, and B. Dkhil, *Phys. Rev. B* **73**, 012102 (2006).

²⁶O. Svitelskiy, D. La-Orautapong, J. Toulouse, W. Chen, and Z.-G. Ye, *Phys. Rev. B* **72**, 172106 (2005); O. Svitelskiy, J. Toulouse, G. Yong, and Z.-G. Ye, *ibid.* **68**, 104107 (2003).

²⁷J. Toulouse, F. Jiang, O. Svitelskiy, W. Chen, and Z.-G. Ye, *Phys. Rev. B* **72**, 184106 (2005); D. La-Orautapong, J. Toulouse, Z.-G. Ye, W. Chen, R. Erwin, and J. L. Robertson, *ibid.* **67**, 134110 (2003).

²⁸B. Mihailova, B. Maier, C. Paulmann, T. Malcherek, J. Ihringer, M. Gospodinov, R. Stosch, B. Gütler, and U. Bismayer, *Phys. Rev. B* **77**, 174106 (2008).

²⁹D. Viehland, S. J. Jang, L. E. Cross, and M. Wuttig, *J. Appl. Phys.* **68**, 2916 (1990).

³⁰D. N. H. Nam, R. Mathieu, P. Nordblad, N. V. Khiem, and N. X. Phuc, *Phys. Rev. B* **62**, 8989 (2000).

³¹E. Vincent, J. Hammann, M. Ocio, J. P. Bouchaud, and L. F. Cugliandolo, in *Complex Behavior of Glassy Systems*, Lecture Notes in Physics Vol. 492, edited by M. Rubi (Springer-Verlag, Berlin, 1997).

³²J. P. Bouchaud, V. Dupuis, J. Hammann, and E. Vincent, *Phys. Rev. B* **65**, 024439 (2001).

³³F. Cordero, F. Craciun, A. Franco, and C. Galassi, *Phys. Rev. B* **74**, 024110 (2006).

³⁴F. Cordero, M. Corti, F. Craciun, C. Galassi, D. Piazza, and F. Tabak, *Phys. Rev. B* **71**, 094112 (2005).

³⁵F. Cordero, F. Craciun, and P. Verardi, *Ferroelectrics* **290**, 141 (2003).

³⁶R. K. Pattnaik and J. Toulouse, *Phys. Rev. B* **60**, 7091 (1999).

³⁷Y. I. Sirotin and M. P. Shaskolskaya, *Fundamentals of Crystal Physics* (Mir, Moscow, 1982).

³⁸M. Adachi, Y. Akishige, K. Deguchi, T. Ikeda, M. Okuyama, A. Sakai, E. Sawaguchi, T. Takenada, T. Tsukamoto, T. Yagi, in *Ferroelectrics and related substances*, Landolt-Börnstein New Series, Group III Vol. 36, Pt. A1 (Springer-Verlag, Heidelberg, 2002).

³⁹Q. M. Zhang and J. Zhao, *Appl. Phys. Lett.* **71**, 1649 (1997).

⁴⁰K. Wieczorek, A. Ziebinska, Z. Ujma, K. Szot, M. Gorny, I. Franke, J. Koperski, A. Soszynski, and K. Roleder, *Ferroelectrics* **336**, 61 (2006); K. Rusek, J. Kruczek, K. Szot, D. Rytz, M. Gorny, and K. Roleder, *ibid.* **375**, 165 (2008).

⁴¹A. Ziębińska, D. Rytz, K. Szot, M. Górný, and K. Roleder, *J. Phys.: Condens. Matter* **20**, 142202 (2008); K. Wieczorek, Z. Ujma, K. Popek, I. Gruszka, M. Górný, J. Koperski, A. Soszynski, and K. Roleder, *ibid.* **21**, 115901 (2009).

⁴²V. S. Vkhnin, R. Blinc, and R. Pirc, *J. Appl. Phys.* **93**, 9947 (2003).

⁴³PNR evolution below a certain temperature which lies tens of degrees above the critical temperature T_c is also considered as the origin of the electrostrictive coupling variation of normal ferroelectrics (see Refs. 40 and 41). However, as it has been pointed out in Ref. 11, an important distinction is that in relaxors the distorted regions develop around a dopant, while in ferroelectrics they arise intrinsically through optic-acoustic mode-mode coupling and they evolve to coalescence into a homogeneously polarized state at T_c .

⁴⁴M. Delgado, E. V. Colla, P. Griffin, M. B. Weissman, and D. Viehland, *Phys. Rev. B* **79**, 140102(R) (2009).